

Electronic Supplementary Material (ESI) for ChemComm.
This journal is © The Royal Society of Chemistry 2016

Supporting information

Unambiguous Characterization of Anisotropic Foldamer Packing in a Foldecture with an Elongated Hexagonal Plate Shape

Eunyoung Yoon, Jintaek Gong, Yoonchul Jung, Wonchul Lee, Russell W. Driver,
and Hee-Seung Lee*

Department of Chemistry, KAIST, Daejeon, 305-701, Korea

E-mail: hee-seung_lee@kaist.ac.kr

Table of Contents

1. Characterization Methods	S2
2. Experimental procedures	S5
3. Characterization results	S8
Figure S1	S7
Figure S2	S8
Figure S3	S9
Figure S4	S9
Figure S5	S10
Figure S6	S10
Figure S7	S11
Figure S8	S11
Figure S9	S12
Figure S10	S12
Figure S11	S13
Figure S12	S13
Figure S13	S14
Figure S14	S14
Figure S15	S15
Figure S16	S17
Figure S17	S19
Table S1	S18
Table S2	S25

1. Characterization Methods

1.1. Nuclear Magnetic Resonance Spectroscopy

NMR samples were prepared by dissolving ca 20 mg peptide in 500 μ L pyridine- d_5 . 1D and 2D ^1H NMR spectra were recorded on a Bruker Avance II 900 MHz NMR spectrometer with a TCi cryoprobe at the Korea Basic Sciences Institute NMR Facility.¹ 2D data were collected in hypercomplex phase-sensitive mode (except for COSY experiments) with a spectral width of 7200 Hz in both dimensions, using 2048 complex data points and 512 t_1 increments with 8 scans per increment.

TOCSY experiments were performed with a dipsi2gpiph pulse sequence (homonuclear Hartman-Hahn transfer using DIPSI2 sequence), COSY experiments with a cosygpqh pulse sequence and ROESY experiments with a roesyegpiph pulse sequence (2D ROESY with cw spinlock for mixing). TOCSY and ROESY spectra were acquired with 60 and 300 ms isotropic mixing times, respectively. Spectra were processed with Mnova NMR software and are referenced to the residual non-deuterated solvent peak. The t_1 dimensions of all 2D spectra were 0-filled to 1024 real data points with 90° phase-shifted QSINE bell window functions applied in both dimensions followed by Fourier transformation and adaptive baseline correction.

1.2. Single crystal X-ray diffraction

Single crystals of peptide **1** were grown from MeOH and diffraction data for **1** were collected on a Bruker D8 QUEST instrument with graphite-monochromated MoK α radiation ($\lambda = 0.71073 \text{ \AA}$) under a stream of N₂ (g) at 122 K. The half-sphere data collection strategy was designed to provide complete data to a maximum resolution of 0.77 \AA ; collection time was 2.5 days. Cell parameters were determined and subsequently refined by SMART.⁶ Data reduction was performed using SAINT.⁷ An empirical absorption correction was applied using the SADABS program.⁸ The structure was solved with direct methods and all nonhydrogen atoms were subjected to anisotropic refinement by full-matrix least-squares on F^2 . Partial occupancy minor disorder components were modeled using CRYSTALS. In general, all non-hydrogen atoms were refined with anisotropic displacement parameters. Hydrogen atoms were generally visible in the difference map and their positions and displacement parameters were refined using restraints prior to inclusion into the model using riding constraints. Peptide **1** was submitted to the CCD (with structure factor file).

¹ Korea basic science Institute, 70, Yuseong-daero 1689 beon-gil, Yuseong-gu, Daejeon, South Korea.

1.3. Synchrotron powder X-ray diffraction

High-resolution of powder X-ray diffracted pattern was collected at SPring-8 (Hyogo, Japan) for structure determination from powder diffraction pattern (SDPD) of self-assembled nano/micro-sized structure, consisted with complex organic molecule. The sample was prepared by our typical self-assembly protocol, followed by drying *in vacuo*, and filled in small glass capillary. Transmission mode with step scanning method was selected at the data collection. The experiment was carried out at room temperature. The radiation wavelength was 0.5000Å. Originally, 2θ data range was 0.01° to 78.0°, but only from 2° to 20° of diffracted data was used in the following SDPD process because of the poor signal-to-noise ratio after 20°.

1.4. AFM

Atomic force microscopy (AFM) images were obtained with Park Systems, XE-100. In order to prepare the sample for the AFM measurement, a drop of peptide solution was placed on a siliconized glass, and was air-dried at room temperature. Non-contact mode was used for the measurement.

1.5. GIWAXS

Grazing incidence wide angle X-ray scattering (GIWAXS) measurements were performed at beamline 3C in the Pohang Accelerator Laboratory (Pohang, Republic of Korea). The GIWAX sample was prepared by dropping on glass (1cm × 1cm). The wavelength of incident X-ray beam was 1.1179Å, and the incidence angle was set to 0.12°.

1.6. TEM

Transmission electron microscope (TEM) measurements were performed with Technai G3 30 at 300kV. TEM specimens were prepared from aqueous solutions of foldectures. The samples were deposited onto 200 mesh carbon coated copper grids from Electron Microscopy Sciences (Hatfield, PA). The sample grids were dried under vacuum and stored in a desiccator before the measurement. The peptide samples were extremely unstable under a focused electron beam, the samples could be only briefly exposed to the electron beam for the recording of the SAED pattern and HRTEM image. It was necessary to repeat numerous times placing defocused electron beam over a fresh plate sample and fast-focusing an electron beam in order to obtain the SAED pattern and HRTEM image.

1.7. SEM

Scanning electron microscope (SEM) images were acquired on Inspect F50, FEI at an accelerating voltage of 10 kV, after Pt coating (sputter coater 108auto, Cressington Scientific Instruments). The prepared dispersion of the assemblages were transferred to a Si wafer and dried under air condition.

1.8. CD

Circular Dichroism (CD) spectra were measured using a Jasco J-815 spectrometer in 1 mm quartz cells in MeOH (0.1 mM). Spectra were recorded from 260 to 190 nm at a scanning rate of 100 nm/min and were averaged 10 scans.

1.9. Out-of-plane and in-plane X-ray diffraction

Out-of-plane and in-plane X-ray diffraction patterns were obtained from a high resolution powder X-ray diffractometer using Philips X'pert ProMPD at KBSI.² Characteristic Cu $K\alpha$ radiation was used as incident beam ($\lambda=1.54178 \text{ \AA}$), and the diffraction patterns were collected at room temperature from 3° to 30° in 2θ range, and the increment was 0.1° .

1.10. Powder X-ray diffraction

PXRD patterns were obtained from a multi-purpose attachment X-ray diffractometer (Rigaku, D/Max-2500) equipped with a pyrolytic graphite (002) monochromator. Characteristic Cu $K\alpha$ radiation was used as an incident beam ($\lambda = 1.54178 \text{ \AA}$) and the diffraction patterns were scanned over 2θ values ranging from 3° up to 30° in increment of 0.1° at room temperature.

² Korea Basic Science Institute, Daegu Center, Daegu, 702–701, Republic of Korea

2. Experimental procedures

2.1. Materials

2.1.1. Solvents and Reagents

All starting reagents were purchased from Sigma-Aldrich, Novabiochem, and Tokyo Chemical Industry (TCI). Dichloromethane (DCM) and *N,N*-dimethylformamide (DMF) were distilled before use. DCM was distilled under N₂ (g) atmosphere in the presence of calcium hydride; DMF was vacuum distilled.

2.1.2. Chromatography

Thin layer chromatography (TLC) was performed on glass plates coated with Merck 60 F254 silica. The visualization was achieved by UV light or by staining with ninhydrin solution. Flash column chromatography was carried out using Merck Kieselgel (230-400 mesh).

2.2. Synthesis

2.2.1. *N*-Boc-(*trans*-(*S,S*)-ACPC)₆-OBn

β -peptide hexamer was prepared from *tert*-butyloxycarbonyl-*trans*-ACPC-benzyl (*N*-Boc-*trans*-(*S,S*)-ACPC)-OBn. The optically pure, doubly protected β -amino acid monomer, *N*-Boc-*trans*-(*S,S*)-ACPC-OBn, was synthesized by literature procedure³. The ACPC hexamer, *N*-Boc-(*trans*-(*S,S*)-ACPC)₆-OBn, was synthesized by the following literature.⁴

2.2.2. *N*-Boc-(*L*)-Leu₂-OBn

To a solution of *N*-Boc-(*L*)-Leu-OH (742 mg, 2.98 mmol) in dry DMF (5 mL), 1-ethyl-3-(3-dimethylaminopropyl)carbodiimide hydrochloride (EDCI·HCl, 686 mg, 3.58 mmol) and *N,N*-diisopropylethylamine (DIEA, 1.56 mL, 8.94 mmol) were added with vigorous stirring. After 30 min, ClNH₃⁺-(*L*)-Leu-OBn (1.00 g, 2.98 mmol) was added, this mixture was stirred at room temperature for 3 h. After completion of the reaction, confirmed by TLC, DMF was removed under vacuum to provide a yellow solid. The solid was dissolved in DCM (10 mL) and washed with aqueous sat. NH₄Cl (3 × 10 mL) solution. The organic layer was dried over MgSO₄, filtered, concentrated *in vacuo*, and purified through flash chromatography eluting with EtOAc/hexane (1/4) to obtain Leu dimer as a white solid (1.16 g, 90 %).

³ P. R. Leplae, N. Umezawa, H. -S. Lee, S. H. Gellman, *J. Org. Chem.*, 2001, **66**, 5629-5632.

⁴ D. H. Appella, L. A. Christianson, D. A. Klein, M. R. Richards, D. R. Powell, S. H. Gellman, *J. Am. Chem. Soc.*, 1999, **121**, 7574-7581.

2.2.3. $\text{ClNH}_3^+ \text{--}((L)\text{-Leu})_2\text{-OBn}$

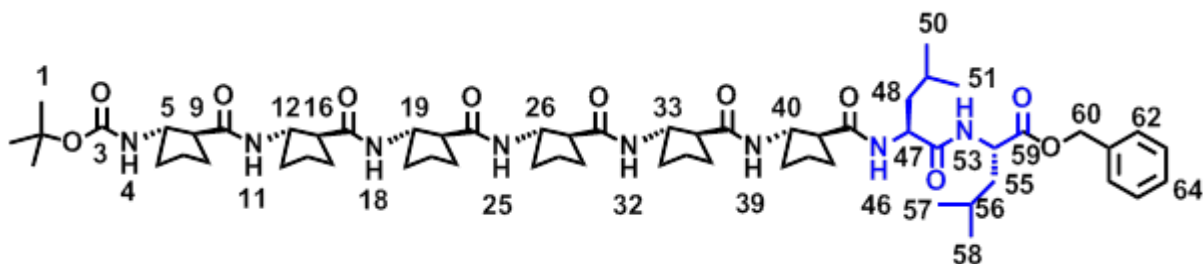
N-Boc-(*L*)-Leu₂-OBn (100 mg, 0.23 mmol) was treated with 4 N HCl in dioxane (5 mL) at 0°C, and the mixture was allowed to warm up to room temperature. After 30 min, the solvent was removed *in vacuo* to yield resulting amine as a hydrogen chloride salt form (85 mg, quant.).

2.2.4. *N*-Boc-(*trans*-(*S,S*)-ACPC)₆-((*L*)-Leu)₂-OBn, **1**

The stirred solution of *N*-Boc-(*trans*-(*S,S*)-ACPC)₆-OBn (874 mg, 1.00 mmol) and 10% Pd/C (88 mg) in dry ethanol (20 mL) was placed under an atmosphere of hydrogen (H₂ (g)) with vigorous stirring. After completion of the reaction, monitored by TLC, the catalyst was removed by filtration through Celite and concentrated *in vacuo* to yield *N*-Boc-(*trans*-(*S,S*)-ACPC)₆-OH as white solid (784 mg, quant.).

To a solution of *N*-Boc-(*trans*-(*S,S*)-ACPC)₆-OH (180 mg, 0.23 mmol) in DMF (5 mL), EDCI·HCl (132 mg, 0.69 mmol) and DMAP (252 mg, 2.07 mmol) were added. After 30 min of stirring, $\text{ClNH}_3^+ \text{--}((L)\text{-Leu})_2\text{-OBn}$ (80 mg, 0.27 mmol) was added, and the mixture was stirred at room temperature for overnight. DMF was removed under vacuum to provide a brown solid. The solid was dissolved in 10 mL of CH₂Cl₂ and washed with sat. NH₄Cl aqueous solution (3 × 10 mL). The organic layers were dried over MgSO₄, filtered, concentrated *in vacuo*, and purified through flash chromatography eluting with CH₂Cl₂/MeOH (95/5) to obtain *N*-Boc-(*trans*-(*S,S*)-ACPC)₆-((*L*)-Leu)₂-OBn as a white crystalline solid (227 mg, 90 %). The powder was further purified by recrystallization from methanol.

2.3. ¹H and ¹³C NMR



¹H NMR (900 MHz, 10 mM, pyridine-d₅, 23°C): 9.51 (1H, d, *J* = 8.0 Hz, H11), 9.35 (1H, d, *J* = 8.5 Hz, H53), 9.19 (1H, d, *J* = 9.1 Hz, H25), 9.16 (1H, d, *J* = 9.6 Hz, H39), 9.13 (1H, d, *J* = 9.1 Hz, H32), 8.96 (1H, d, *J* = 8.0 Hz, H18), 8.55 (1H, d, *J* = 9.2 Hz, H23), 8.42 (1H, d, *J* = 8.0 Hz, H4), 7.54 (2H, d, *J* = 7.8 Hz, H62), 7.36 (2H, t, *J* = 7.8 Hz, H63), 7.21 (1H, t, *J* = 7.2 Hz, H64), 5.34 (1H, d, *J* = 12.6 Hz, H60), 5.27 (1H, d, *J* = 12.6 Hz, H60), 5.26 (1H, m, H54), 5.07 (2H, m, H47, H40), 4.82 (1H, quintet, *J* = 8.4, H33), 4.78 (1H, quintet, *J* = 8.4, H26), 4.74 (2H, m, H12, H19), 4.51 (1H, quintet, *J* = 7.6, H5), 3.28 (1H, m, H44), 2.92 (2H, m, H23, H30), 2.85 (1H, quartet, *J* = 8.0, H37), 2.78 (1H, quartet, *J* = 8.4, H9), 2.68 (1H, quartet, *J* = 8.8, H16), 2.59 (1H, m, H55), 2.52 (1H, m, H43), 2.34 (1H, m, H36), 2.33 (1H, m, H29), 2.31 (1H, m, H22), 2.24 (1H, m, H49), 2.23 (1H, m, H17), 2.22 (1H, m, H8), 2.19 (1H, m,

H56), 2.16 (1H, m, H34), 2.16 (1H, m, H27), 2.14 (1H, m, H48), 2.10 (1H, m, H6), 2.09 (1H, m, H34), 2.09 (1H, m, H20), 2.08 (1H, m, H48), 2.08 (1H, m, H56), 2.05 (1H, m, H13), 2.04 (1H, m, H41), 1.98 (1H, m, H8), 1.96 (1H, m, H27), 1.96 (1H, m, H43), 1.95 (1H, m, H36), 1.95 (1H, m, H28), 1.92 (1H, m, H41), 1.91 (1H, m, H29), 1.89 (1H, m, H7), 1.87 (1H, m, H20), 1.86 (1H, m, H17), 1.87 (1H, m, H22), 1.85 (1H, m, H42), 1.85 (1H, m, H21), 1.83 (1H, m, H35), 1.80 (1H, m, H35), 1.79 (1H, m, H28), 1.75 (1H, m, H6), 1.74 (1H, m, H21), 1.74 (1H, m, H7), 1.72 (1H, m, H42), 1.70 (1H, m, H13), 1.59 (1H, m, H14), 1.95 (1H, m, H14), 1.55 (9H, s, H1), 1.07 (3H, d, $J = 6.7$ Hz, H57/H58), 1.04 (3H, d, $J = 6.7$ Hz, H57/H58), 1.01 (3H, $J = 7.0$ Hz, H50/H51), 0.97 (3H, $J = 7.0$ Hz, H50/H51).

^{13}C NMR (100 MHz, 10 mM, pyridine- d_5 , 23°C): 176.40(C10), 176.31(C45), 176.05(C17), 175.93(C31), 175.68(C38, C24), 174.80(C52), 173.76(C59), 157.60(C3), 137.57(C61), 129.27(C66, C62), 129.56(C65, C63), 128.51(C64), 79.78(C2), 66.89(C60), 58.71(C5), 56.56(C33), 56.43(C19), 56.38(C26), 56.35(C12), 56.01(C40), 55.29(C16), 54.39(C9), 54.26(C47), 54.21(C30), 53.42(C23), 53.10(C37), 52.75(C44), 52.01(C54), 42.35(C48), 40.80(C55), 34.91(C41), 34.38(C27), 34.25(C20), 34.01(C6), 33.74(C34), 33.32(C13), 30.55(C15), 30.16(C29), 30.11(C8), 30.00(C43), 29.86(C22), 29.42(C36), 29.12(C1), 26.75(C42), 26.10(C7), 26.10(C7), 25.91(C14), 25.70(C21, C28), 25.67(C35), 25.24(C56), 25.03(C49), 24.12(C51), 24.00(C50), 22.15(C58), 21.97(C57).

HRMS: (ES $^{+}$): found (1123.6726); $\text{C}_{60}\text{H}_{92}\text{N}_8\text{O}_{11}$, $[\text{M} + \text{H}^{+}]$ requires 1123.42

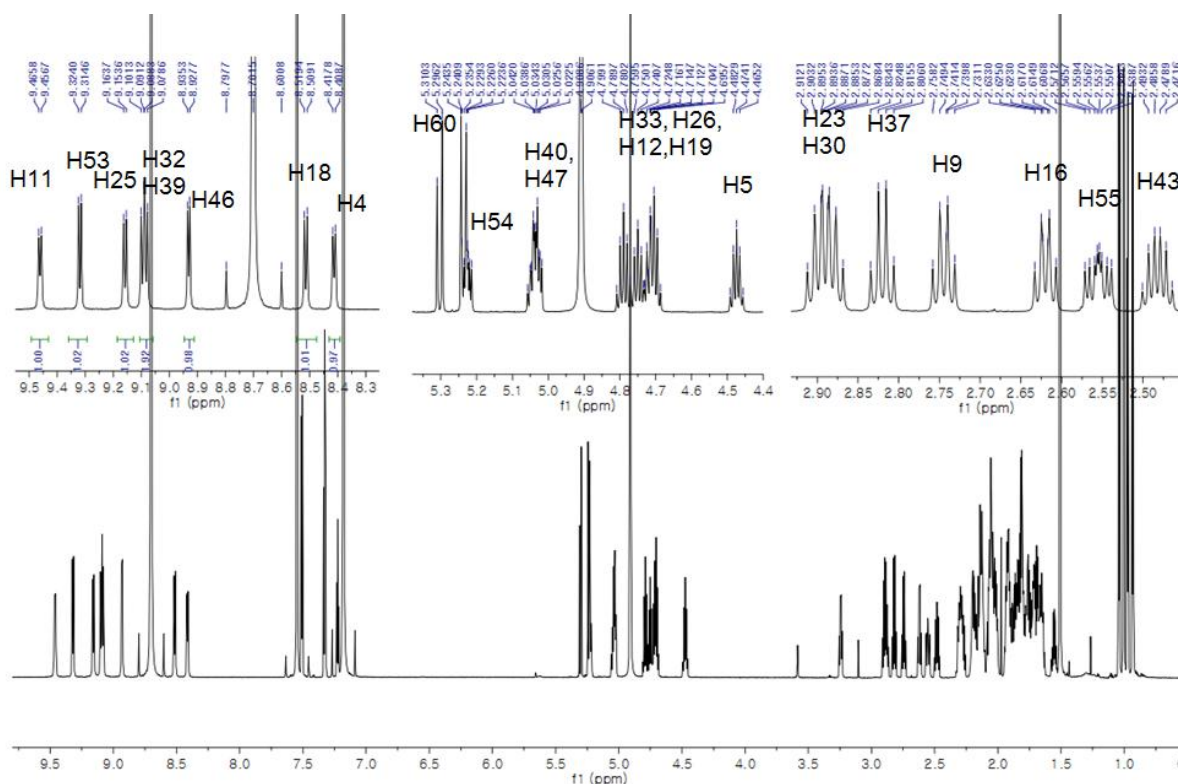


Figure S1. ^1H NMR spectrum (900 MHz, 10 mM, pyridine- d_5 , 23°C) and proton assignment for **1**.

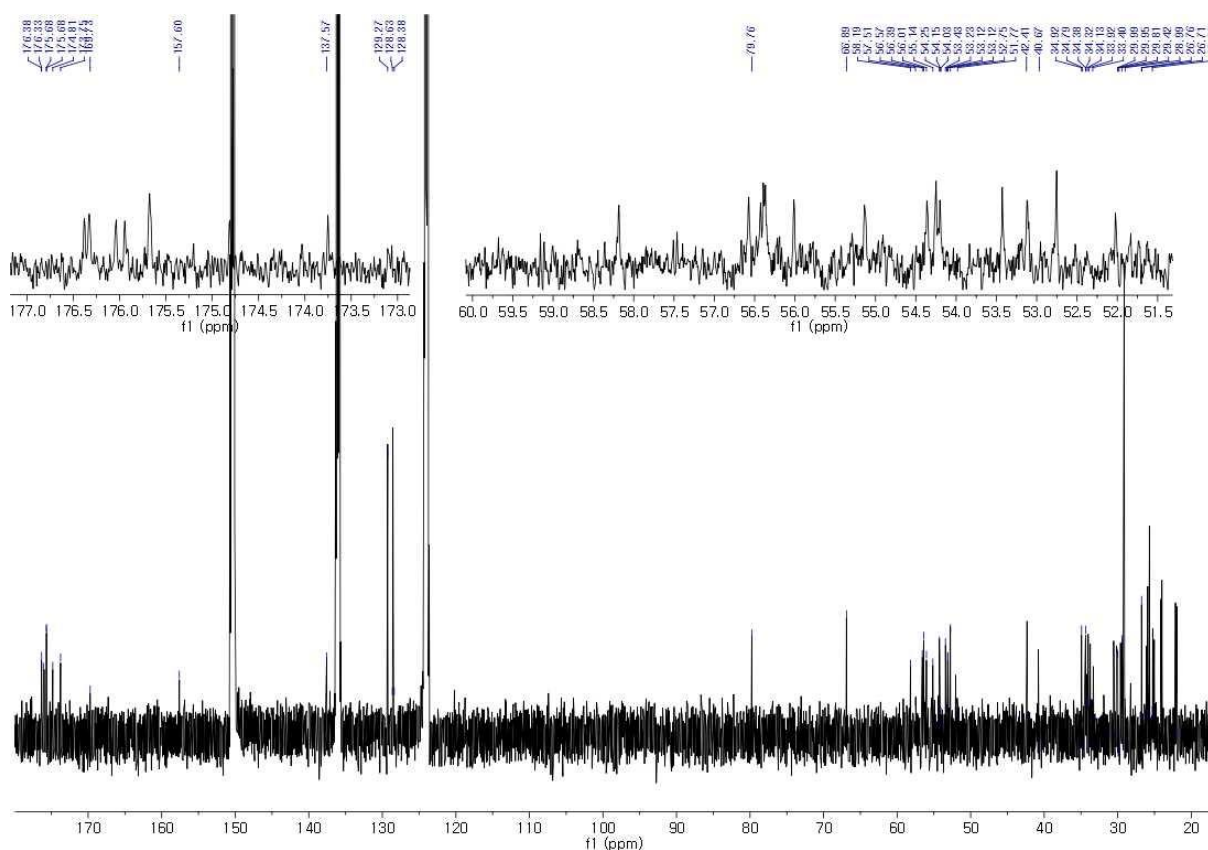


Figure S2. ^{13}C NMR spectrum (100 MHz, 10 mM, pyridine-d_5 , 23°C) for **1**.

2.4. Self-assembly of **1**

A solution of **1** in THF ($200\ \mu\text{L}$, $1\ \text{gL}^{-1}$) was rapidly injected to an aqueous solution of P123 ($1\ \text{mL}$, $0 - 8\ \text{gL}^{-1}$) with vigorous stirring for 1 min at room temperature. Then the mixture was allowed to be aged for 3 h at the same room temperature without stirring. The resulting solution was centrifuged, and the supernatant was decanted. The remaining white precipitates were washed with distilled water ($3 \times 1\ \text{mL}$)

3. Structural Characterization

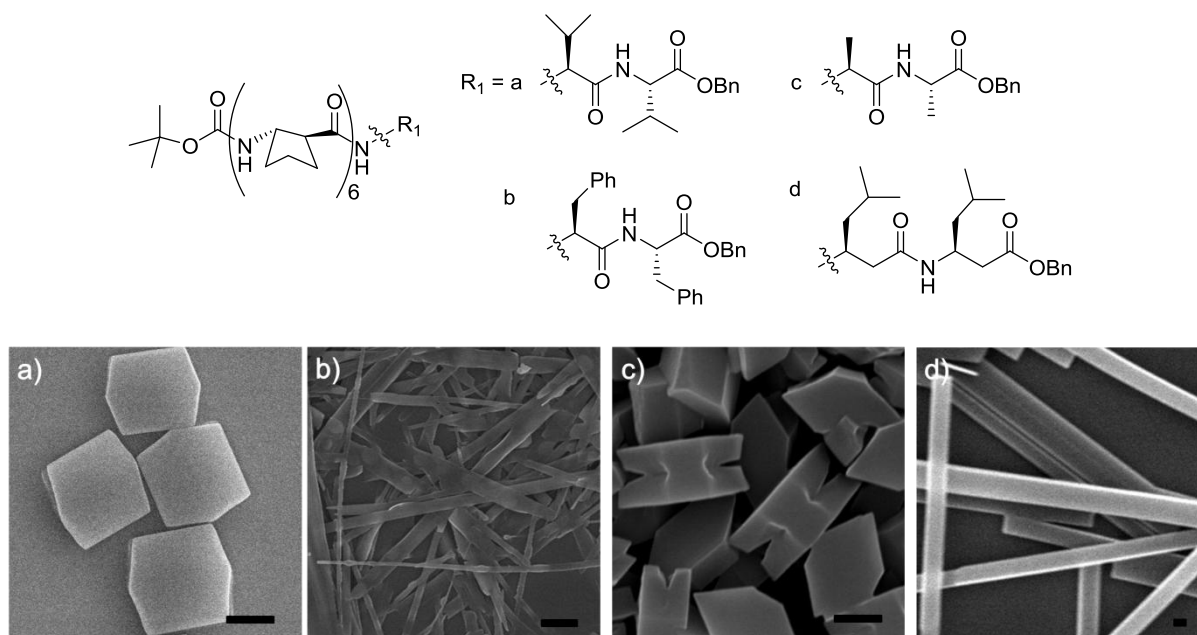


Figure S3. SEM images of graft foldamers composed of ACPC hexamer and α -(*L*)-amino acid dimers (R₁) (a) valine, (b) phenylalanine, (c) alanine, (d) β -leucine. Scale bars : 1 μm .

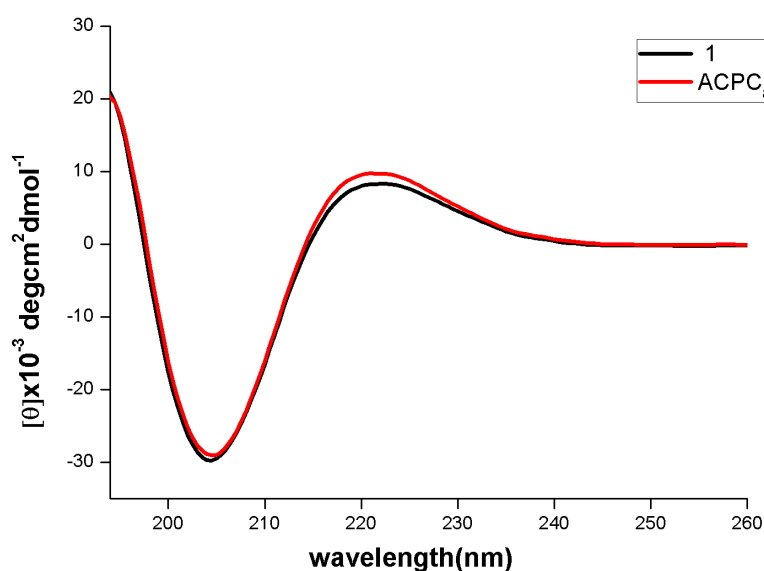


Figure S4. CD spectra in MeOH for a 0.1 mM solution of **1**(black) and ACPC₈(red). The lineshape indicates that **1** adopts a stable right-handed 12-helical secondary structure. Two peptides Boc-((*S,S*)-ACPC)₈-OBn and Boc-((*S,S*)-ACPC)₆-(*L*)Leu₂-OBn have similar CD patterns.

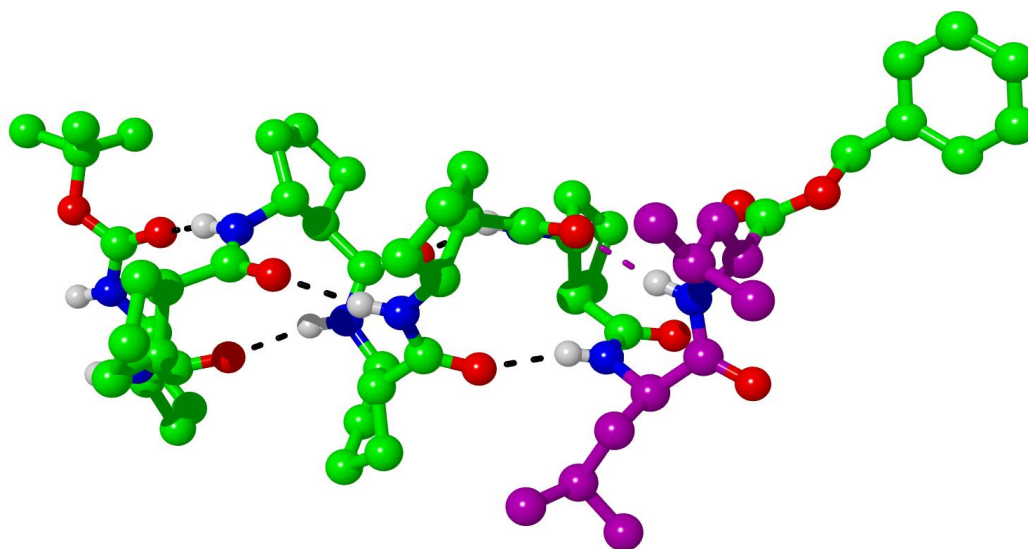


Figure S5. Single crystal of **1** obtained from MeOH showing a 12-helical ACPC region (hydrogen bonds as black dotted lines) and an 11-membered hydrogen bonding (purple dotted line) at the end of the helix in solid state. Leucine residues are purple.

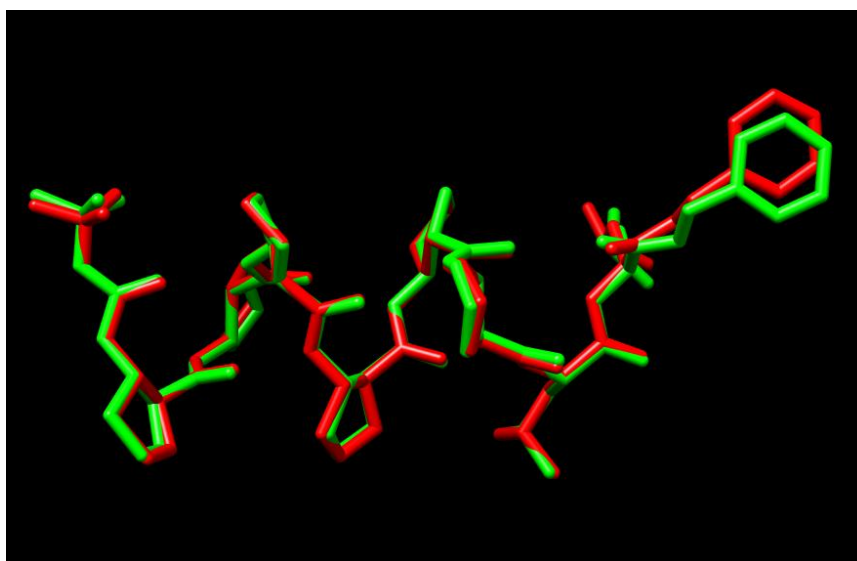


Figure S6. The overlay image between molecular structure of single crystal (red) and PXRD (green) result. The small RMSD value (0.116\AA for 30 atoms in the backbone structure) indicates similarity between the two structures.

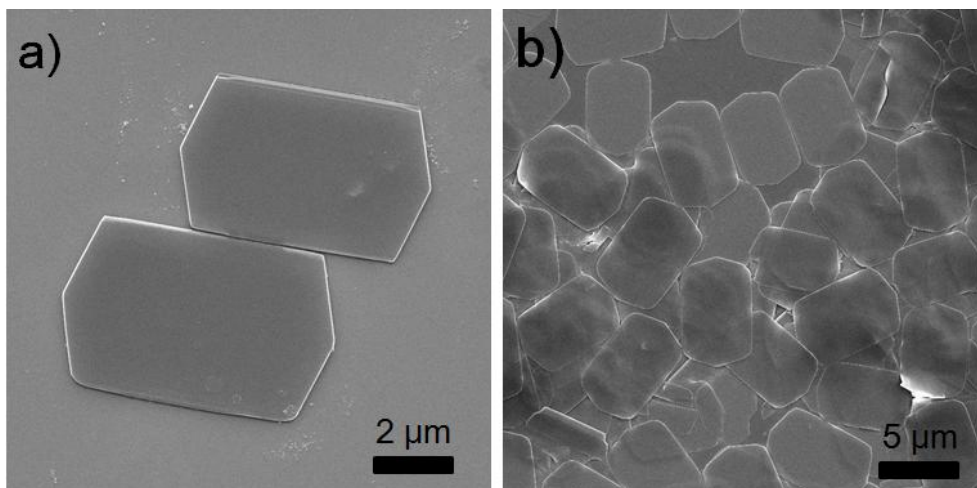


Figure S7. (a) (b) SEM images of foldectures from **1**, prepared at P123 1 gL⁻¹.

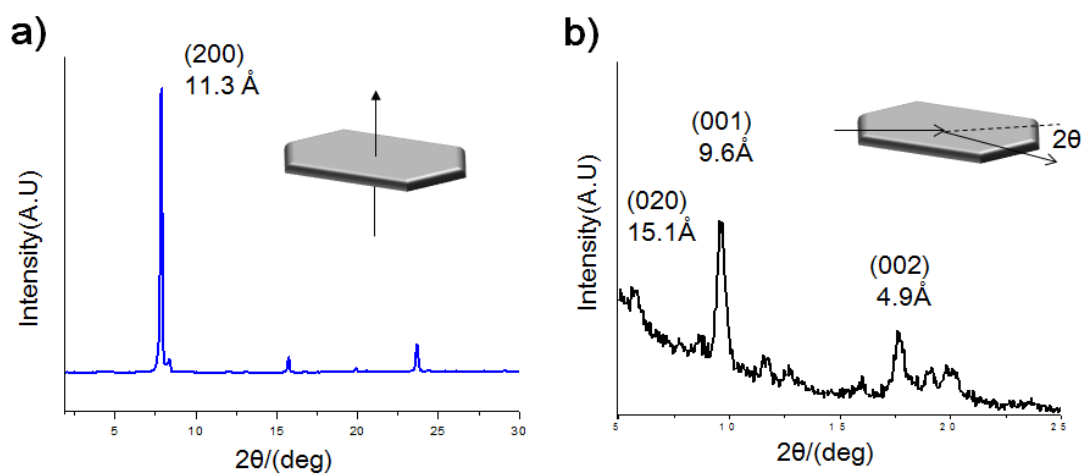


Figure S8. Out-of-plane and in-plane XRD data of plate morphology **P₁**. (a) Out-of-plane XRD pattern and (b) In-plane XRD pattern of **P₁**. Indexed planes and its corresponding *d*-space values are represented, respectively.

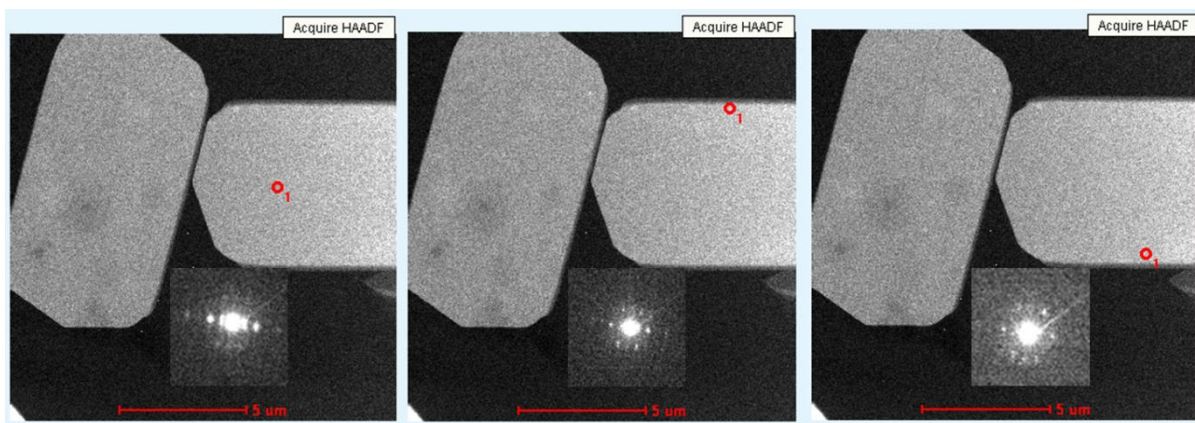


Figure S9. SAED patterns of P_1 using scanning TEM. The same SAED patterns were obtained at three different points.

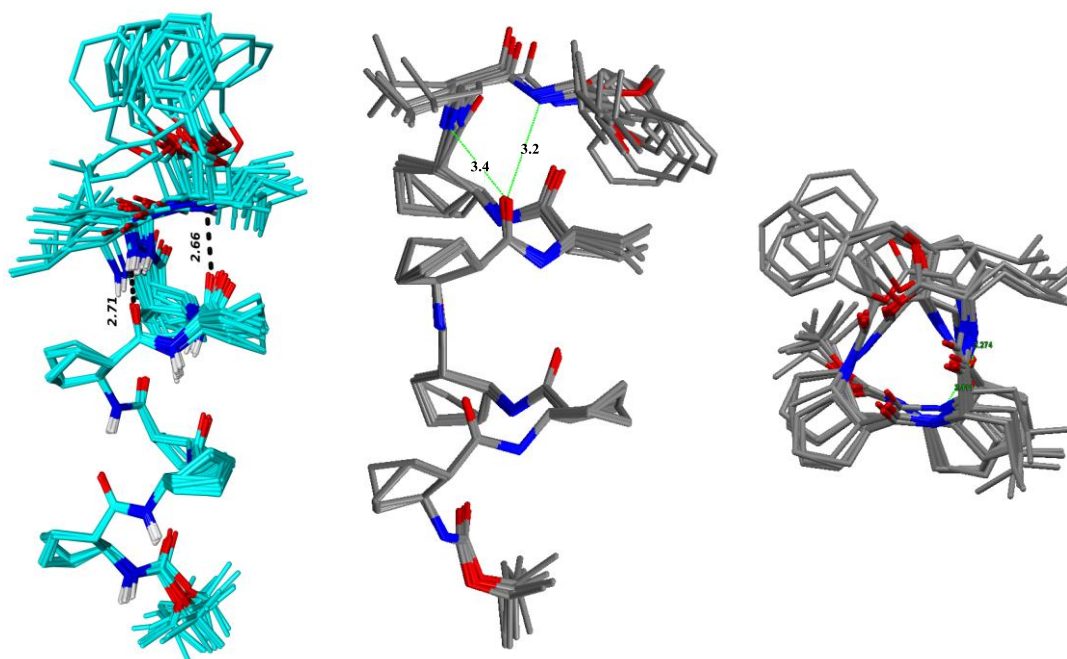


Figure S10. Comparison of major (aqua) and minor (grey) solution-state conformers of **1**. The minor is positioned to form a 12- and 15-membered hydrogen bonding (12/15 macrocycle⁵).

⁵ Reminiscent of a Schellman loop: (a) A. R. Viguera, L. Serrano, *J. Mol. Biol.*, 1995, 150–160. (b) S. Datta, N. V. Uma, N. Shamala, P. Balaram, *Biopolymers*, 1999, **50**, 13–22.

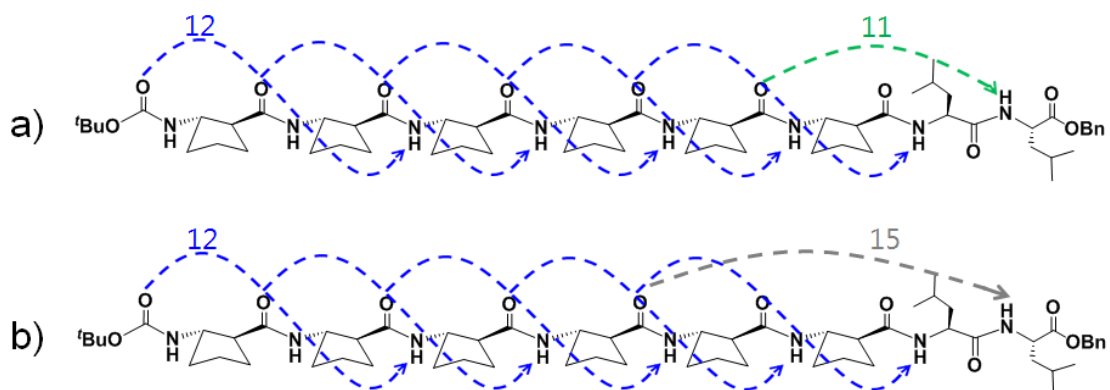


Figure S11. Intermolecular hydrogen bonding of **1** from the a) major b) minor solution-state structures. Blue; 12-membered hydrogen bonding, Green; 11-membered hydrogen bonding, Gray; 15-membered hydrogen bonding.

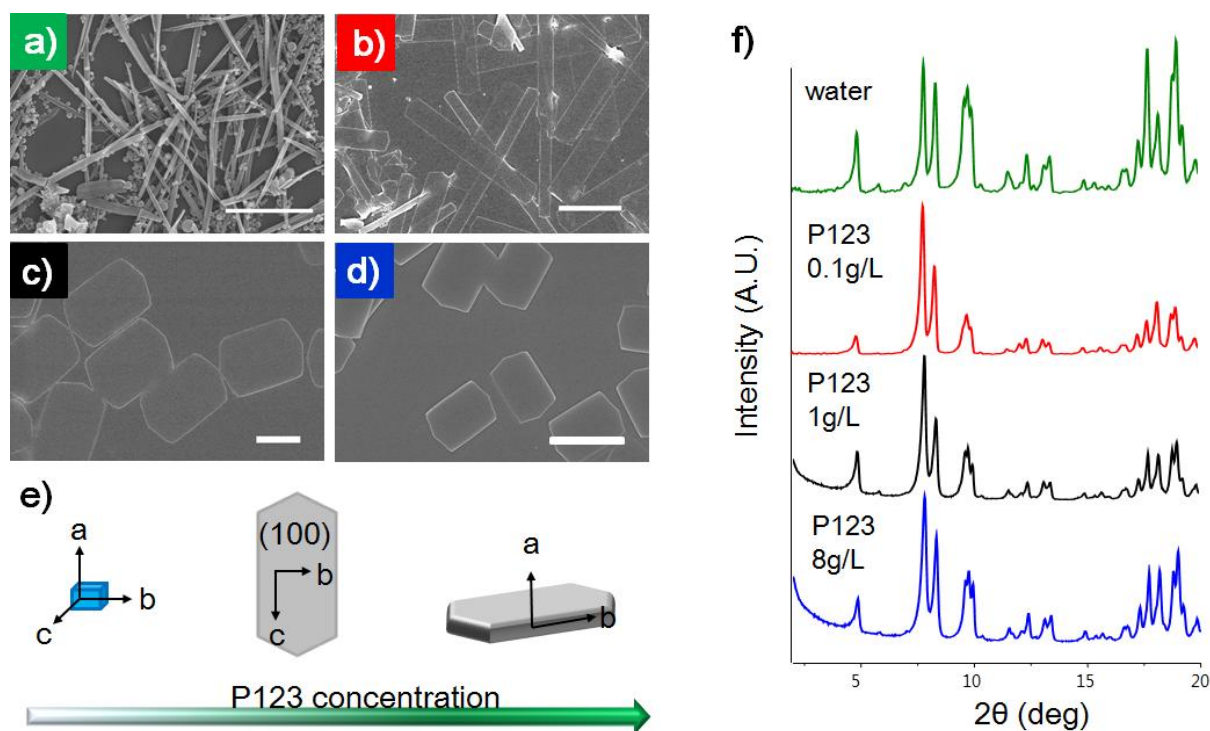


Figure S12. SEM images of **P1** from P123 concentrations (a) 0.0 gL⁻¹ (distilled water) (b) 0.1 gL⁻¹ (c) 1 gL⁻¹ and (d) 8 gL⁻¹, respectively. (e) Schematic representation of predicted growth morphology depending on various P123 concentrations. (f) PXRD patterns of the self-assembled structures of **1** from various P123 concentrations.

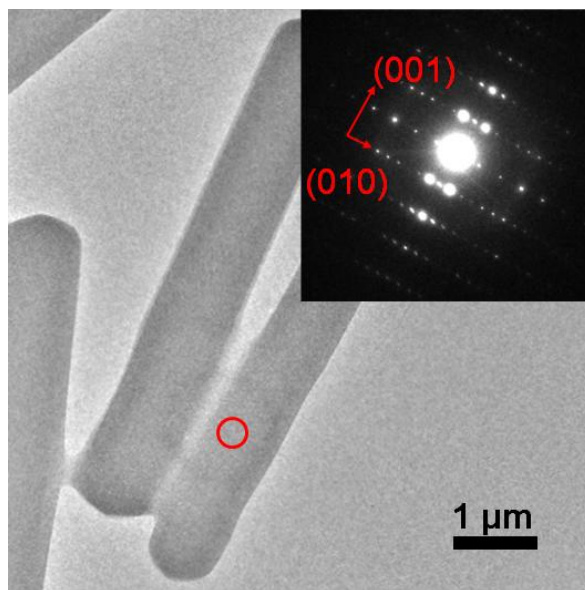


Figure S13. TEM image and SAED pattern (inset) of foldecture of **1** from P123 0.1 gL⁻¹. The SAED pattern was indexed to the same plane with **P**₁, so that suggesting their essentially identical molecular packing mode. The measured distance from electron diffraction analysis are 15.1, 4.9 Å, which matches well with the observed *d* spacing (010),(001) plane.

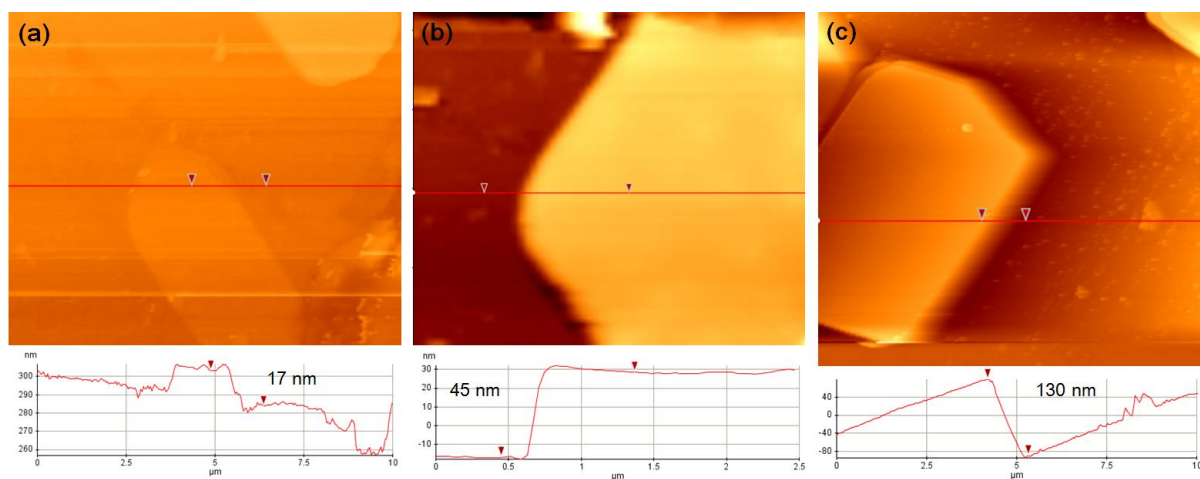


Figure S14. AFM images with height line profiles of foldectures of **1** from different P123 concentrations, (a) 0.1 gL⁻¹, (b) 4 gL⁻¹ and (c) 8 gL⁻¹, respectively. The thickness were measured to be about (a) 17 nm, (b) 45 nm (c) 130 nm, respectively.

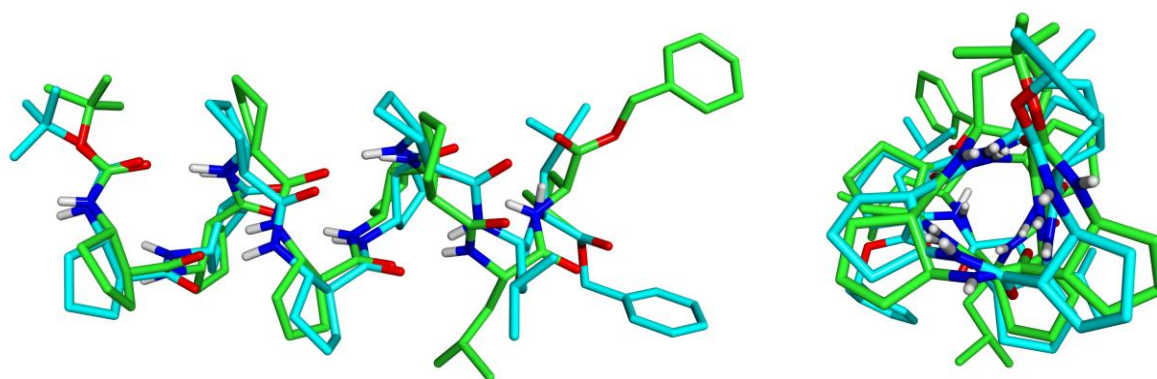


Figure S15. Comparison of single-crystal X-ray structure (green) and representative solution-state NMR-calculated major conformer (cyan) of **1**.

4. PXRD

4.1. Unit cell determination

Semi-automated indexing program, *Crysfire*⁶ was used to determine unit cell parameters of this foldecture. More than 50 peaks were selected for the peak indexing process. As a result, an orthorhombic unit cell was obtained with the acceptable figure-of-merit value (F.O.M.=15.44). The space group for this structure was decided to $P2_12_12$. The obtained cell was further refined to $a=22.5473(5)$, $b=30.2016(5)$, $c=9.63661(18)$, and $\alpha = \beta = \gamma = 90^\circ$ during the process.

4.2. Structure Calculation

For the structure calculation, *F.O.X.*⁷ program was used. To insert the molecular model in this program, single-crystal's molecule was prepared as Fenske-Hall Z-matrix file using *OpenBabel*⁸ software. Restraints for all bond distances and angles were set up based on the statistical values from the Cambridge Crystallographic Data Centre (CCDC) database including intramolecular hydrogen bonds (some torsional angles, as well). Several dihedral angles, especially for protecting groups or leucine's side residues, were restricted to move. Anti-bump parameters were applied depending on Van der Waals radius of each atomic species, thus dynamical occupancy correction was not used. Global B_{iso} parameter was turned on to be refined. During the calculation, parallel tempering algorithm was applied to the system, and more than 10,000,000 cycles of calculation were proceeded. Other parameters for the global optimization were remained as the program's default values. As a results, the molecular packing structure was successfully obtained, used for the initial structure for the following Rietveld refinement.

4.3. Rietveld refinement

The refinement process was preceded using *GSAS/EXPGUI*⁹ program. Before the refinement of atomic parameters, whole profile fitting in $F_{(calc)}$ weighted (Model biased) manner was preceded. For the profile function, Pseudo-Voigt profile¹⁰ was used in order to fit asymmetric shape of peaks at low angle range. All bond lengths and angles were restrained by statistical values from the CCDC database. These restraints were kept until the last stage of this refinement. Temperature displacement factors were not allowed to be refined separately, so that the degree of freedom was controlled effectively.

⁶ R. Shirley, *The CRYSFIRE System for Automatic Powder Indexing: User's Manual*, The Lattice Press, 41 Guildford Park Avenue, Guildford, Surrey GU2 7NL, England, 2000.

⁷ V. Favre-Nicolin and R. Černý, *Zeitschrift für Kristallographie, International journal for structural, physical, and chemical aspects of crystalline materials*, 2004, **219**, 847-856.

⁸ N. O'Boyle, M. Banck, C. James, C. Morley, T. Vandermeersch and G. Hutchison, *J Cheminform*, 2011, **3**, 1-14.

⁹ B. H. Toby, *Journal of Applied Crystallography*, 2001, **34**, 210-213.

¹⁰ P. Thompson, D. E. Cox and J. B. Hastings, *Journal of Applied Crystallography*, 1987, **20**, 79-83.

One of the most difficult question of this refinement was prediction of the expected preferred orientation texture. Nevertheless the sample was consisted with tightly packed thin-plates, the sample was filled at the cylindrical holder. Therefore, it was become almost impossible to designate the preferred orientation in manner of Miller indices. Thus, we decided to apply the Spherical Harmonic (ODF) preferential orientation approximation model, which is included in *EXPGUI* program as a module, to this structure¹¹. Spherical harmonic order was set to 6 for the cylindrical sample symmetry. The refined ODF terms and coefficients are as follows.

(2,0,0)=-0.0552, (2,0,2)=-0.2253, (4,0,0)=0.0603, (4,0,2)=0.0384, (4,0,4)=0.1659, (6,0,0)=0.3160, (6,0,2)=-0.0916, (6,0,4)=0.2816, (6,0,6)=0.1967, and the texture index=1.0318.

A great development was achieved in the pattern fitting with 1.0318 value of texture index, representing the existence of moderate preferred orientation texture in the sample.¹². After several thousands of cycles, the final structure was obtained with following *R*-factors, $R_{wp}=0.0436$, $R_p=0.0313$. The final Rietveld plot is presented at Figure S5. The detail experimental parameters are presented at Table S1.

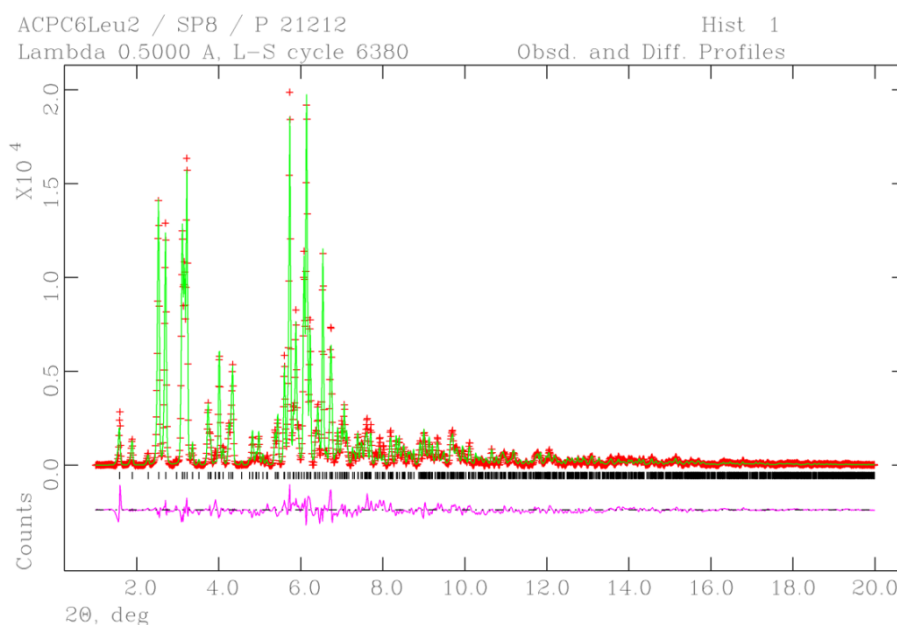


Figure S16. The final Rietveld plot of the foldecture. The plot was prepared by *powplot* module, included in *EXPGUI* program. (Red crosses; obtained diffracted spots, green solid line; calculated diffracted pattern, magenta solid line; difference function, black tick-marks; expected Bragg position)

¹¹ B. H. Toby, *op. cit.*

¹² (a) J. A. Kaduk, J. W. Reid, K. Zhong, A. M. Gindhart and T. N. Blanton, *Powder Diffr.*, 2015, **30**, 211-217.
 (b) J. A. Kaduk, K. Zhong, A. M. Gindhart and T. N. Blanton, *Powder Diffr.*, 2015, **30**, 205-210.

Table S1. Experimental details for the PXRD analysis

Crystal data	
Chemical formula*	C ₆₀ N ₈ O ₁₁
M_r^*	1008.70
Cell setting, space group	Orthorhombic, $P2_12_12$
Temperature (K)	298
a, b, c (Å)	22.5473(5), 30.2016(5), 9.63661(18)
α, β, γ (°)	90, 90, 90
V (Å ³)	6562.21(22)
Z	4
Radiation type	Synchrotron radiation ($\lambda=0.5000\text{Å}$)
Specimen form, colour	Powder (particle morphology: small thin plate), white
Specimen preparation temperature (K)	Room temperature
Data collection	
Diffractometer	Spring-8 synchrotron Beamline
Data collection method	Specimen mounting: glass capillary, Mode: transmission, Scan method: step
2θ (°)	$2\theta_{\min} = 1.0$, $2\theta_{\max} = 20.0$, increment = 0.01
Refinement	
Refinement on	Intensities
R factors and goodness-of-fit	$R_p = 0.0313$, $R_{wp} = 0.0436$, $R_{exp} = 0.0178$, $S = 2.49$
Excluded region(s)	None
Profile function	Pseudo-voigt
No. of parameters	248
H-atom treatment*	Omitted
$(\Delta/\sigma)_{\max}$	0.10
* H-atoms were omitted during the structure determination process.	

5. Solution state structure characterization

5.1. Distance, Angle and Hydrogen Bonding Restraints

Distance restraints were derived from ROESY spectra obtained at 298 K. ROE cross-peaks were collected manually and classified as very strong, strong, medium, medium weak, weak or very weak (see ROE crosspeak table for distances). Where diastereotopic/anisochronous protons could not be assigned, pseudoatom corrections were applied.¹³ Distances for each restraint category were calibrated by averaging known proton-proton interatomic distances. Upper distance limits for sidechain protons were generous to prevent the exclusion of legitimate conformations. Beta amino acid amide dihedral angle restraints ($\pm 30^\circ$) were derived $^3J_{\text{NH-H}\beta}$ coupling constants *via* the Karplus Equation.¹⁴ A *cis* geometry was enforced for all amide bonds. Hydrogen bond restraints with a square-well potential were applied based on amide proton variable temperature coefficients, hydrogen/deuterium isotope exchange rates and ^1H chemical shifts versus random coil values.

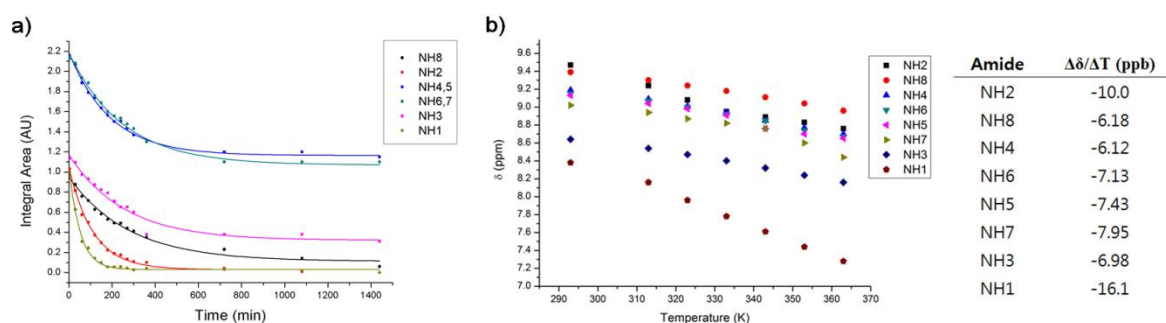


Figure S17. Hydrogen bonding information was obtained using temperature-dependent chemical shifts of the amide proton resonances. The temperature dependent proton spectra were measured between 298 K and 365 K in 10 K temperature steps. Deuterium/Hydrogen isotope exchange of the amide protons was studied on a 400 MHz instrument by dissolving **1** in C_5NH_5 (0.5 mL) and H_2O (50 μL). (a) ^1H NMR NH/D exchange curves for amide protons in C_5NH_5 added D_2O at 25 $^\circ\text{C}$. (b) Amide proton NMR chemical shift temperature dependence (ppm/K) for **1** in C_5NH_5 .

5.2. Calculation

Calculations were performed with Xplor-NIH 2.35¹⁵ using modified topology and parameter sets incorporating ACPC residues plus peptide terminus modifications. Molecular topology and parameter files were created *de novo*. Calculation proceeded by a modified conjugate

¹³ K. Wuthrich, M. Billeter, W. Braun, *J. Mol. Biol.* 1983, **169**, 949-961.

¹⁴ M. Karplus, *J. Am. Chem. Soc.* 1963, **85**, 2870-2871.

¹⁵ (a) C. D. Schwieters, J. J. Kuszewski, N. Tjandra, G. M. Clore. *J. Magn. Res.*, 2003, **160**, 66-74. (b) C. D. Schwieters, J. J. Kuszewski, G. M. Clore, *Progr. NMR Spectroscopy*, 2006, **48**, 47-62.

gradient algorithm¹⁶ with very slow cooling. NOE, distance, dihedral and improper violations were observed and average structures calculated by standard files provided within the distribution.

The NMR-data calculated conformational ensemble was bimodal. 38 (of 50) structures without violations (no dihedral angle violations > 3.0° nor NOE violations > 0.3 Å nor improper violations > 4.0° Å nor bond length violations > 0.05 Å) were ranked in energy. The lowest 30 were superimposed and subsequently partitioned into two distinct families of conformers containing 22 and 5 structures, respectively, using the ensemble cluster function¹⁷ in UCSF Chimera.¹⁸ Following analysis, the entire procedure was repeated from a different randomized starting geometry; the results were nearly identical.¹⁹ Publication quality images were created using Pymol.²⁰

5.3. Hydrogen Bonding Restraints

Calculations without any hydrogen bonding restraints (but including NOEs and Karplus restraints) produced a set of canonical 12-helical secondary structures through the beta amino acid residues. An (*i*→*i*+3) intramolecular hydrogen bonding scheme consistent with VT, H/D, amide proton chemical shift NMR studies and NOE patterns was subsequently employed to restrain the first five residues of *N*-Boc-((*S,S*)-ACPC)₆-(Leu)₂-OBn during refinement. In order to avoid prejudice, no hydrogen bonding restraints were applied to residues seven or eight.

(residue partners)		(distance)	-range	+range
resid 1 BocO	resid 3 N	2.9	0.1	0.5
resid 1 O	resid 4 N	2.9	0.1	0.5
resid 2 O	resid 5 N	2.9	0.1	0.5
resid 3 O	resid 6 N	2.9	0.1	0.5

¹⁶ M. J. D. Powell, *Mathematical Programming*, 1977, **12**, 241-254.

¹⁷ L. A. Kelley, S. P. Gardner, M. J. Sutcliffe, *Protein Eng.*, 1996, **11**, 1063-1065.

¹⁸ E. F. Pettersen, T. D. Goddard, C.C. Huang, Couch, G. S, D. M. Greenblatt, E. C. Meng, T. E. Ferrin, *J. Comput Chem.*, 2004, 1605-1612.

¹⁹ RWD thanks Roger Midmore for fruitful discussions regarding simulated annealing.

²⁰ The PyMOL Molecular Graphics System, Version 1.7.4 Schrödinger, LLC.

5.4. Torsional Angle Restraints

Torsional angle restraints about the HN-N-CB-HB dihedral derived from the Karplus equation were applied to ACPC residues with a range of $\pm 30^\circ$.

residue 1 $^3J_{\text{HN-H}\beta} = 8.3 \text{ Hz}$; HN-N-CB-HB = $157.0^\circ \pm 30.0^\circ$.

residue 2 $^3J_{\text{HN-H}\beta} = 8.0 \text{ Hz}$; HN-N-CB-HB = $153.0^\circ \pm 30.0^\circ$.

residue 3 $^3J_{\text{HN-H}\beta} = 9.2 \text{ Hz}$; HN-N-CB-HB = $170.0^\circ \pm 30.0^\circ$.

residue 4 $^3J_{\text{HN-H}\beta} = 9.1 \text{ Hz}$; HN-N-CB-HB = $167.0^\circ \pm 30.0^\circ$.

residue 5 $^3J_{\text{HN-H}\beta} = 9.1 \text{ Hz}$; HN-N-CB-HB = $167.0^\circ \pm 30.0^\circ$.

residue 6 $^3J_{\text{HN-H}\beta} = 9.6 \text{ Hz}$; HN-N-CB-HB = $176.0^\circ \pm 30.0^\circ$.

For the final calculation, leucine 7 was excluded from the left-handed helical region of Ramachandran space²¹. The phi angle of leucine 8 was not restrained. The psi angle (ψ , $\text{N}_i - \text{C}_{\alpha i} - \text{C}_i - \text{N}_{(i+1)}$) was restrained in neither leucine 7 nor leucine 8.

residue 7 $^3J_{\text{HN-H}\alpha} = 6.90 \text{ Hz}$; HN-N-C-HA = $-70.0^\circ \pm 50.0^\circ$.

residue 8 $^3J_{\text{HN-H}\alpha} = 8.00 \text{ Hz}$; not restrained.

5.5. NOE Crosspeak Table and Distance Definitions

Experimental NMR Distance Restraints from ROESY

900 MHz Instrument 20 μM , 24°C, pyridine-D₅

Identification of ROE crosspeaks was complicated by extensive overlap within the ^1H spectrum. Amide protons (5 + 6), H β protons (3+2), H α protons (3+4), H α and H β (7+6) and virtually all H γ , H δ and H ϵ were overlapped. At the C-terminus long-range ROE a few crosspeaks consistent with unfolded geometries were observed but not included in the structure calculation.

(ROE crosspeak number) = (+ range, - range)

8,7 = 2.8 (0.5, 0.4) 6 = 3.2 (0.4, 0.6) 5,4 = 3.7 (0.4, 0.7)

3 = 4.5 (0.7, 0.7) 2 = 5 (0.7, 0.7) 1 = 6 (0.7, 0.7)

63 intramolecular NOEs

18 short range intermolecular NOEs

19 medium/long range intermolecular NOEs

²¹ G. N. Ramachandran, V. Sasiskharan, *Adv. Protein Chem.*, 1968, **23**, 283–437.

!HN-HN INTERMOLECULAR CROSSPEAKS

resid 8	HN resid 7	HN	3.7	0.4	0.7	!	5
resid 8	HN resid 6	HN	5.0	0.7	0.7	!	2

!HN-HB (i, i-1) INTERMOLECULAR CROSSPEAKS

resid 2	HN resid 1	HB	4.5	0.7	0.7	!	3
resid 3	HN resid 2	HB	3.2	0.4	0.6	!	6
resid 4	HN resid 3	HB	4.5	0.7	0.7	!	3
resid 5	HN resid 4	HB	4.5	0.7	0.7	!	3
resid 6	HN resid 5	HB	4.5	0.7	0.7	!	3

!HN-HB (i, i-2) INTERMOLECULAR CROSSPEAKS

resid 3	HN resid 1	HB	3.7	0.4	0.7	!	4
resid 4	HN resid 2	HB	5.0	0.7	0.7	!	2
resid 5	HN resid 3	HB	5.0	0.7	0.7	!	2
resid 6	HN resid 4	HB	6.0	0.7	0.7	!	1
resid 7	HN resid 5	HB	3.7	0.4	0.7	!	5
resid 8	HN resid 6	HB	5.0	1.0	1.7	!	

!HN-HB (i, i-3) INTERMOLECULAR CROSSPEAKS

resid 4	HN resid 1	HB	4.5	0.7	0.7	!	3
resid 8	HN resid 5	HB	3.7	0.4	0.7	!	4

!HN-HA (i, i-1) INTERMOLECULAR CROSSPEAKS

resid 2	HN resid 1	HA	2.8	0.4	0.4	!	8
resid 3	HN resid 2	HA	2.8	0.4	0.4	!	8
resid 4	HN resid 3	HA	2.8	0.4	0.4	!	8
resid 5	HN resid 4	HA	2.8	0.4	0.4	!	8
resid 6	HN resid 5	HA	2.8	0.4	0.4	!	8
resid 7	HN resid 6	HA	2.8	0.4	0.4	!	8
resid 8	HN resid 7	HA	3.2	0.4	0.6	!	6

!HN-HA (i, i+1) INTERMOLECULAR CROSSPEAKS

resid 7	HN resid 8	HA	5.0	0.7	0.7	!	2
---------	------------	----	-----	-----	-----	---	---

!HN-HA (i, i-2) INTERMOLECULAR CROSSPEAKS

resid 3	HN resid 1	HA	5.0	0.7	0.7	!	2
resid 7	HN resid 5	HA	1.0	1.0	1.0	!	1
resid 8	HN resid 6	HA	5.0	0.7	0.7	!	2

!HN-HA (i, i-3) INTERMOLECULAR CROSSPEAKS

resid 5 HN resid 2 HA 5.0 0.7 0.7 ! 2

!HA-HA (i, i-1) INTERMOLECULAR CROSSPEAKS

resid 6 HA resid 5 HA 5.0 0.7 0.7 ! 2

!HB-HA (i, i-1) INTERMOLECULAR CROSSPEAKS

resid 5 HB resid 4 HA 4.5 0.7 0.7 ! 3

!HB-HA (i, i-2) INTERMOLECULAR CROSSPEAKS

resid 4 HB resid 6 HA 2.8 0.5 0.3 ! 7

resid 2 HB resid 4 HA 2.8 0.5 0.3 ! 7

resid 3 HB resid 5 HA 2.8 0.5 0.3 ! 7

resid 1 HB resid 3 HA 2.8 0.5 0.3 ! 7

! MISC INTERMOLECULAR CROSSPEAKS

resid 8 HB* resid 5 HB 3.7 0.5 1.7 ! 4

! Benzyl INTERMOLECULAR CROSSPEAKS

resid 8 HE* resid 7 HA 5.0 0.5 2.5 ! 2

resid 8 HZ* resid 7 HA 5.0 0.5 2.5 ! 1

! INTRAMOLECULAR CROSSPEAKS

! Residues 1-6

!Observed and inferred; distance ranges are larger than intermolecular cross-peaks

resid X HA resid X HE* 3.2 1.6 1.6 !

resid X HA resid X HD* 3.8 1.6 1.6 !

resid X HA resid X HG* 3.7 1.6 1.6 !

resid X HB resid X HE* 3.7 1.6 1.6 !

resid X HB resid X HD* 3.7 1.6 1.6 !

resid X HB resid X HG* 2.8 1.6 1.6 !

resid X HN resid X HA 3.2 0.4 0.6 !6/5

resid X HN resid X HB 3.2 0.4 0.6 !6/5

resid X HB resid X HA 3.2 0.4 0.6 !6/5

!Leucine 7

resid 7 HB* resid 7 HA 3.2 0.4 1.0 ! 6

resid 7 HB* resid 7 HN 3.2 0.4 1.0 ! 6

resid 7 HN resid 7 HA 3.2 0.4 0.6 ! 6

resid 7 HA resid 7 HD1* 5.0 0.4 2.6 ! 2

!Leucine 8

resid 8	HB*	resid 8	HA	3.2	0.4	1.0	! 6
resid 8	HB*	resid 8	HN	3.2	0.4	1.0	! 6
resid 8	HN	resid 8	HA	3.2	0.4	0.6	! 6
resid 8	HA	resid 8	HD1*	5.0	0.4	2.6	! 2
resid 8	HB*	resid 8	HD1*	5.0	0.4	3.0	! 2

Table S2. Crystallographic Parameters, Data Collection and Refinement for Single Crystal of **1**.

<i>Single Crystal data</i>	
CCDC 1446030	$V = 6446.7 (3) \text{ \AA}^3$
$\text{C}_{60}\text{H}_{92}\text{N}_8\text{O}_{11}$	$Z = 4$
$M_r = 1125.71$	Mo $K\alpha$ radiation
Orthorhombic, $P2_12_12$	$\mu = 0.08 \text{ mm}^{-1}$
$a = 22.4000 (9) \text{ \AA}$	$T = 122\text{K}$
$b = 29.9961 (13) \text{ \AA}$	$0.70 \times 0.20 \times 0.20 \text{ mm}$
$c = 9.5945 (4) \text{ \AA}$	
<i>Data collection</i>	
Bruker Kappa Apex2 diffractometer	7710 reflections with $I > 2.0\sigma(I)$
Absorption correction multi-scan	$R_{\text{int}} = 0.044$
SADABS (Siemens, 1996)	
$T_{\text{min}} = 0.98, T_{\text{max}} = 0.98$	$\theta_{\text{max}} = 27.6^\circ$
169900 measured reflections	8060 independent reflections
<i>Refinement</i>	
$R[F^2 > 2\sigma(F^2)] = 0.051$	H atoms treated by a mixture of independent and constrained refinement
$wR(F^2) = 0.133$	$\Delta\rho_{\text{max}} = 0.37 \text{ e \AA}^{-3}$
$S = 0.94$	$\Delta\rho_{\text{min}} = -0.26 \text{ e \AA}^{-3}$
8050 reflections	Absolute structure: NA
769 parameters	Absolute structure parameter: NA
386 restraints	